Rock and Soil Mechanics

Volume 44 | Issue 8 Article 7

12-6-2023

Optimal strut position of deep foundation pit with convex corner under surcharge of adjacent building

Bao-guo CHEN
Faculty of Engineering, China University of Geosciences, Wuhan, Hubei 430074, China,
baoguo_chen@126.com

Zeng-pan JIA
Faculty of Engineering, China University of Geosciences, Wuhan, Hubei 430074, China,
zengpan_jia@126.com

Follow this and additional works at: https://rocksoilmech.researchcommons.org/journal

 Part of the Geotechnical Engineering Commons

Recommended Citation

CHEN, Bao-guo and JIA, Zeng-pan (2023) "Optimal strut position of deep foundation pit with convex corner under surcharge of adjacent building," *Rock and Soil Mechanics*: Vol. 44: Iss. 8, Article 7.
DOI: 10.16285/j.rsm.2023.00112
Available at: https://rocksoilmech.researchcommons.org/journal/vol44/iss8/7

This Article is brought to you for free and open access by Rock and Soil Mechanics. It has been accepted for inclusion in Rock and Soil Mechanics by an authorized editor of Rock and Soil Mechanics.

Optimal strut position of deep foundation pit with convex corner under surcharge of adjacent building

Abstract

Since the mechanical behavior of the convex corner is complex due to surcharge near the excavation, it is of great importance to evaluate the influence of changes in strut position on the convex corner. Field monitoring and numerical simulations were used to analyze the influence law of the changes of strut position on the deformation and stress characteristics of the convex corner area. The axial force of inner strut, the lateral earth pressure on the pile, the horizontal displacement of the pile, the settlement of adjacent building and the bending moment of the pile were obtained. The research results show that the depth of strut position that is too high or too low is unfavorable to the coordinated deformation and the force of the retaining system. In contrast, the optimal strut position in this analysis is between 0.33 and 0.50 times the depth of the excavation (0.10–0.33 times the depth of the pile).

Keywords

deep foundation pit, convex corner, strut position, surcharge

This article is available in Rock and Soil Mechanics: https://rocksoilmech.researchcommons.org/journal/vol44/iss8/7

Rock and Soil Mechanics 2023 44(8): 2400−2408 ISSN 1000−7598
https://doi.org/10.16285/j.rsm.2023.00112 http://rocksoilmech.researchcommons.org/journal

Optimal strut position of deep foundation pit with convex corner under surcharge of adjacent building

CHEN Bao-guo, JIA Zeng-pan
Faculty of Engineering, China University of Geosciences, Wuhan, Hubei 430074, China

Abstract: Since the mechanical behavior of the convex corner is complex due to surcharge near the excavation, it is of great importance to evaluate the influence of changes in strut position on the convex corner. Field monitoring and numerical simulations were used to analyze the influence law of the changes of strut position on the deformation and stress characteristics of the convex corner area. The axial force of inner strut, the lateral earth pressure on the pile, the horizontal displacement of the pile, the settlement of adjacent building and the bending moment of the pile were obtained. The research results show that the depth of strut position that is too high or too low is unfavorable to the coordinated deformation and the force of the retaining system. In contrast, the optimal strut position in this analysis is between 0.33 and 0.50 times the depth of the excavation (0.10–0.33 times the depth of the pile).
Keywords: deep foundation pit; convex corner; strut position; surcharge

1 Introduction

In recent years, the foundation pit is characterized by deep excavation and large scale, with adjacent buildings close by in China[1–2]. For deep excavation, the inner strut can effectively restrain the displacement of retaining structure of foundation pit and ensure the safety and orderly operation of foundation pit[3]. Due to the restriction by the surrounding environment and land use red line, surcharge and convex corner certainly exist in the practical projects.

The complex interaction between the adjacent buildings and the foundation pit leads to a series of problems such as adjacent building deformation[4–7], ground settlement[8–10] and soldier pile deflection[11–12]. In addition, the excavation surfaces at the convex corner weaken the restraining effect between the soils that may induce the stress concentration and excessive deformation. Wang et al.[13] and Song et al.[14] used numerical simulations to study the deformation characteristics of the convex corner area and found that the deformation of the retaining structure near the convex corner was large. Wu et al.[15] and Pan et al.[16] found that the axial force of soil nail and the displacement of the foundation pit at the convex corner increased significantly. These studies considering the surcharge and the convex corner provide valuable guidance for designing the support and for the construction of deep foundation pits. However, most of the above studies were focused on the displacement and force characteristics of deep excavation with fixed strut position. These studies seldom consider the impact of changes in the strut position on convex corner under adjacent loads.

For the above foundation pits reinforced with the struts, the removal and abandonment of the temporary support structure will cause the waste of resources and prolong the construction period of the project. Hence, the retaining structures and inner struts of the foundation pit retaining system can be used for the structural exterior wall and structural floor of the underground structure, respectively[17]. Nevertheless, the strut position does not necessarily coincide with the floor slab position of the underground structure in actual project. If the strut position in the foundation pit subjected to adjacent building loads has been changed without authorization, the stress redistribution of the soil outside the foundation pit will cause the stress and deformation of the pit to differ from the original design values, which will also result in inestimable impact on the whole foundation pit system.

The stress state and deformation of the foundation pit vary with the inner strut length[18–20]. Similarly, the variation of inner strut position will also affect the displacement of the retaining structure and the inner force[21–24]. Gao et al.[25] also found that the position of steel inner strut had a great influence on the axial force of concrete strut in multi-braced retaining situation. However, these studies only considered one aspect of force or deformation of the foundation pit, and the analysis of coordinated deformation and force of the whole retaining system was ignored. Therefore, further studies are urgently needed to adequately support actual engineering requirements.

In the present study, the effect of inner strut position variation on a deep foundation pit with convex corner under the condition of adjacent loads was evaluated. The displacement of the retaining structure, the horizontal earth pressure on the soldier pile, the axial force of the inner strut, the bending moment of the soldier pile, and the settlement and inclination of adjacent buildings were investigated through field monitoring and numerical simulation. The range of optimum strut position, the algebraic

Received: 8 March 2023 Accepted: 1 May 2023
This work was supported by the National Natural Science Foundation of China (52178370) and the Research Fund of Sinohydro Bureau 7 Co., Ltd. (STT-SJQ-SG0022020-KY-001).
First author: CHEN Bao-guo, male, born in 1981, PhD, Associate Professor, research interests: soil–structure interaction. E-mail: baoguo_chen@126.com
Corresponding author: JIA Zeng-pan, male, born in 1994, Master, Assistant engineer, focusing on the soil–structure interaction. E-mail: zengpan_jia@126.com

relationship between the strut position and the deformation of the retaining structure and the adjacent building were analyzed to guide the actual engineering activities.

2 Engineering problem analysis

2.1 Project overview

The foundation pit studied covers an area of approximately 2.75 × 10^4 m^2, with an excavation depth and circumference of 17.5 m and 750 m, respectively (Fig. 1(a)). According to the engineering investigation reports, the stratigraphic sequence from top to bottom associated with the site includes a miscellaneous fill, silty clay, silty clay with breccia, strongly weathering argillaceous siltstone, conglomerate, and limestone. The corresponding soil layer parameters are obtained based on field investigation and indoor soil parameter experiment, as listed in Table 1. Groundwater primarily occurs as stagnant water in the upper layer of the mixed fill and as karst fissure water in the lower rocks. The dewatering wells in the foundation pit are used for dewatering and the collection wells around the foundation pit are arranged to drain the water. Before and after the soil excavation, the groundwater level in the foundation pit was approximately 1 m below the bottom. There is a building near the convex corner, with a height of approximately 20 m and a distance from the edge of the foundation pit of 6 m (Fig. 1(b)).

2.2 Retaining system

In this project, the support method integrates the cast-in-place pile and local concrete inner strut/anchor cable/double-row piles. The foundation pit support illustrated in Fig. 1 involves the section *AC* representing the single-row pile and an anchor cable support, the section *CE* involving the single-row pile and internal strut, the section *EF* reflecting a double-row pile support, the section *FG* associated with a double-row pile support and an inner strut, and the section *GA* representing a double-row pile support. The slope ratio at the top of the foundation pit is 1:1.

The single-row piles utilized are ϕ1 000 mm @ 1 500 mm cast-in-place piles, while the double-row piles are ϕ1 000 mm@1 500 mm cast-in-place piles with spacing of the front and back rows equal to 3 m. In addition, the pile length is 25 m. The borehole diameter, spacing, length, and angle of the prestressed anchor cables are 150 mm, 1 500 mm, 16 m, and 15°, respectively. The free section lengths of the first, second, and third prestressed anchor cables are correspondingly 7.0 m, 5.0 m, and 5.0 m; the anchor section lengths are 9.0 m, 10.0 m, and 11.0 m; and the prestresses are 85 kN, 90 kN, and 80 kN, respectively. The inner strut section measures 800 mm × 1 000 mm, and the concrete inner strut is rigidly connected to the soldier pile. The specific parameters of retaining structure are listed in Table 2.

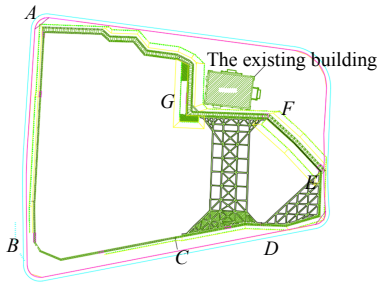

(a) Plan view of foundation pit

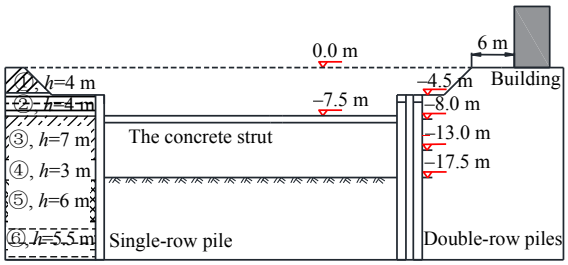

(b) Profile of section *FG*

Fig. 1 Layout of foundation pit

Table 1 Soil parameters

Stratum	Elastic modulus /MPa	Poisson's ratio μ	Internal friction angle /(°)	Cohesion /kPa	Density /(kg · m^{-3})	Thickness /m
Miscellaneous fill	8	0.38	15	8	1 850	4
Silty clay (plastic)	13.3	0.33	10	20	1 860	4
Silty clay (low plastic)	14.3	0.32	14	31	1 910	7
Silty clay (non-plastic)	14.6	0.32	16	40	1 960	3
Silty clay with breccia	11.6	0.34	20	28	1 900	6
Strongly weathered argillaceous sandstone	150	0.25	25	35	2 180	6
Conglomerate	150	0.25	35	39	2 180	6
Limestone	200	0.22	50	35	2 480	−

Table 2 Parameters of retaining structure

Structure type	Material	Elastic modulus /MPa	Poisson's ratio μ	Density /(kg · m^{-3})
Pile	C35	3.0×10^4	0.2	2 420
Concrete strut	C35	3.0×10^4	0.2	2 420
Anchor cable	Q235	2.1×10^5	0.3	7 500

2.3 Excavation of foundation pit and layout of monitoring points

The settlement of the adjacent building was measured using a DNA03 leveling instrument, and the inclinometer tube was used to measure the horizontal displacement of the soldier piles, and the inner force in the soldier piles was determined using an embedded JMZX-215 concrete strain gage. The monitoring points CX14-CX17 were used to measure the settlement of the adjacent building, which were installed around the corners of the building. The monitoring points ZH18, ZH20 and ZH22 were installed in the front piles of the double-row pile to measure the horizontal displacement of the piles. The monitoring points ZC04, ZC05 and

ZC06 were used to measure the axial force, which were arranged on the inner struts. The specific monitoring points and locations are shown in Fig. 2. The specific construction conditions of the deep excavation are listed in Table 3.

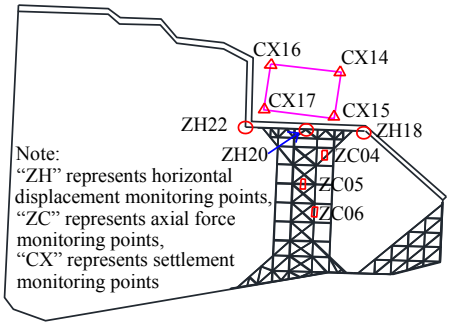

Fig. 2 Layout of monitoring points

Table 3 Construction procedures

Construction step	Detail description	Excavation depth/m
Case 1	Construct the double-row piles and single-row piles	—
Case 2	Excavate the first layer of soil	0 to –4.5
Case 3	Set up the first row of anchor cable and internal strut	—
	Excavate the second layer of soil	–4.5 to –8
Case 4	Set up the second row of anchor cable	—
	Excavate the third layer of soil	–8 to –13
	Set up the third row of anchor cable	—
Case 5	Excavate the fourth layer of soil to the base of foundation pit	–13 to –17.5

3 Analysis of field monitoring results

3.1 Horizontal displacement of piles

The horizontal displacements of the front piles are shown in Fig. 3. The monitoring point ZH22 measures the largest horizontal displacement, with a value of 24.56 mm, and the overall sequence of the horizontal displacement for these piles is ZH22 > ZH20 > ZH18. Obviously, the convex corner area is unfavorable for controlling the horizontal displacement of piles. The horizontal displacement in the convex corner point is larger than that in the middle of excavation surface and the displacement associated with the internal corner. The horizontal displacements of the soldier pile are approximately in arch shape at the monitoring points ZH20 and ZH18, since the strut has a great limiting effect on the horizontal displacement. However, the maximum value of horizontal displacement in the convex corner occurs at the pile top, owing to the increase in excavation faces at the convex corner and lack of inner strut, which weakens the restraining effect and leads to the stress concentration and consequently excessive deformation. These indicate that the convex corner area is the principal deformation area of the excavation pit.

3.2 Axial force

The variation of support axial force with the excavation depth is shown in Fig. 4. It is clearly demonstrated that the monitoring point ZC04 measures the largest axial force, with a value of approximately 2 800 kN, and the sequence of the axial force for these struts is ZC04 > ZC05 > ZC06. In addition, the axial forces measured by the monitoring points ZC04-ZC06 increase with the excavation depth, but the growth rate of axial force gradually decreases.

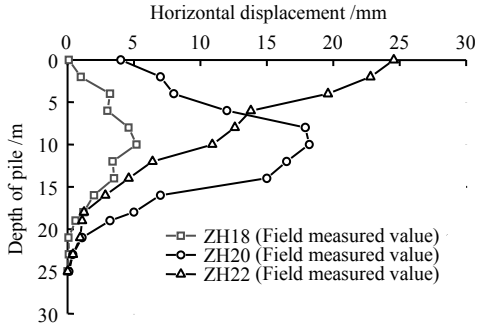

Fig. 3 Horizontal displacements of soldier piles

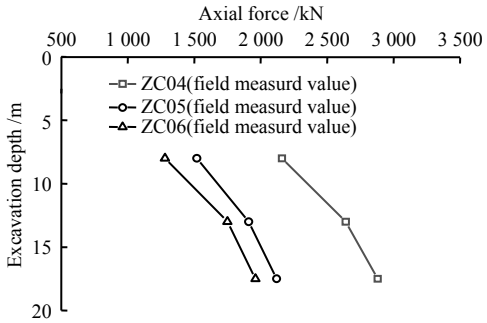

Fig. 4 Axial forces of struts

3.3 Settlement of the building

The settlement of the adjacent building is shown in Fig. 5. Evidently, as the excavation depth increases, the monitoring point CZ17 measures the largest vertical displacement, with a value of approximately 10.40 mm, and the overall sequence for these monitoring points of the adjacent building is CZ17 >CZ15 >CZ16 >CZ14. Due to the fact that the settlement measured by the monitoring point CZ17 is larger than that measured by CZ15, it is enough to prove that the settlement of convex corner area is larger than that of the middle of excavation face. In addition, the maximum differential settlement of the building is 5.61 mm, and the tilt rate of the building is 0.17‰.

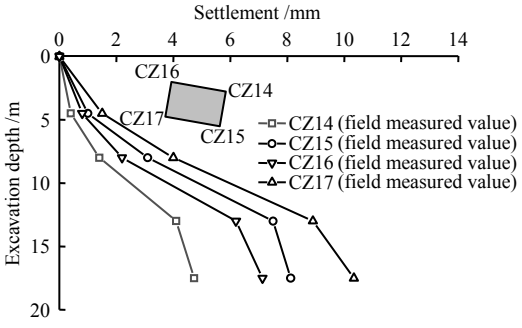

Fig. 5 Settlements of the building

4 Numerical simulation

4.1 Numerical model and parameters

Based on the geometric and engineering geological conditions of the foundation pit, the software ABAQUS[26–27] was used to simulate the actual project, and the numerical model is shown in Fig. 6. The vertical boundaries of the model is constrained by fixing the horizontal displacements, while the bottom boundary is fixed in both vertical and horizontal directions. The height of the model is about 4.0 times the depth of foundation pit H_e (= 17.5 m), while the length and width are both 10.0 times the H_e. Thus, the size of the model is 175 m×175 m×70 m.

In the finite element model, a three-dimensional (3D) 8-node entity reduction integral element (C3D8R) is used to discretize the soil, and the soil is considered as an elastoplastic material that satisfies the Mohr–Coulomb criterion. The soil parameters are listed in Table 1. The pile rows are equivalent to a wall based on the bending rigidity, the specific thicknesses of single- and double-row piles are 785 mm and 1 570 mm, respectively. Pile rows, inner struts, and anchor cables are considered as linearly elastic materials and associated with elastic models, and the parameters of the soil and retaining structures are listed in Table 2. The diaphragm wall is represented by solid element, while the anchor cables and the internal struts are represented by beam element. The soil, inner struts, anchor rods, and soldier piles are linked through binding contacts to simulate the slippage between soil and structures, the normal relation of the contact element at the pile–soil interface is hard contact, the tangential relation of that is the friction contact, and the finite sliding is adopted at the pile–soil contact interface. In the model, the building load is simplified to a uniform load on the convex corner area, and the construction process is consistent with the actual project.

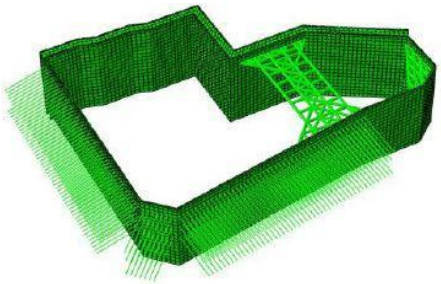

Fig. 6 3D numerical model

4.2 Numerical simulation validation

The overall deformation law of the foundation pit is illustrated in Fig. 7. Figure 8 shows the comparison results of field monitoring and numerical simulation. The numerical simulation results exhibit the same tendency as the field monitoring data. The differences in maximum horizontal displacement of the soldier piles measured by the monitoring points ZH18, ZH20 and ZH22 are 3.8%, 6.2%, and 4.0%, respectively. The differences in maximum axial force of the inner struts measured by the monitoring points ZC04, ZC05 and ZC06 are 3.4%, 2.8%, and 2.1%, respectively. Regarding the building settlement, the differences in maximum vertical displacement measured by the monitoring points CZ14, CZ15, CZ16 and CZ17 are 6.0%, 4.7%, 1.4%, and 2.0%, respectively.

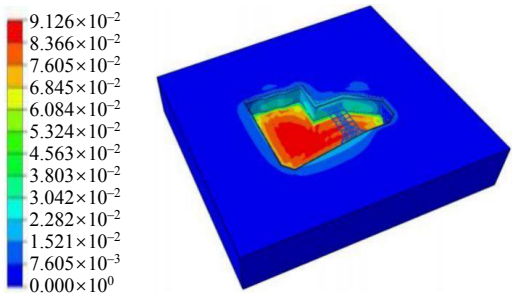

Fig. 7 Overall displacement field of foundation pit (unit: m)

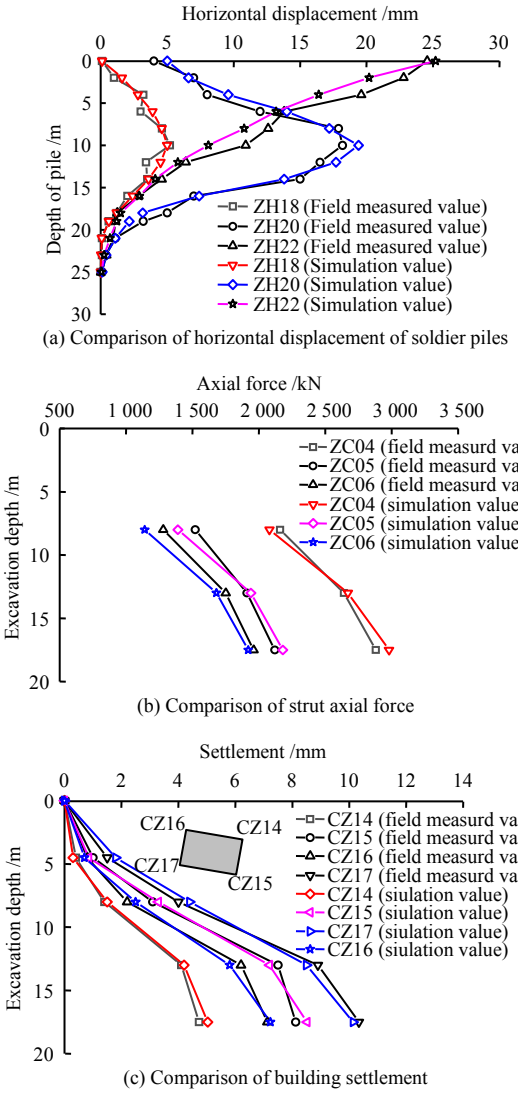

Fig. 8 Comparisons of simulated and measured values

Therefore, the field monitoring data validate the numerical simulation results. The validated numerical model can be utilized to reveal the impact of changes in the inner strut position on the deformation and

stress of the foundation pit.

5 Analysis of stress and deformation associated with inner strut position change

In this analysis, the strut position is moved upwards or downwards 3 m in each case. Thus, in the following analysis, "±0" represents the strut at the original position, and the vertical distance between the strut and the pile top is 3 m; "–3" represents that the strut moves upwards 3 m, and the vertical distance between the strut and the pile top is 0 m; "+3" represents that the strut moves downwards 3 m, and the vertical distance between the strut and the pile top is 6 m.

5.1 Horizontal displacement

As shown in Figs. 9 and 10, under the condition of inner strut depths of 0 m, 3 m and 6 m, the horizontal displacement variations at monitoring points ZH18, ZH20 and ZH22 are not the same. At the inner strut depth of 0 m, the horizontal displacement patterns do not alter at the monitoring points ZH18, ZH20 and ZH22 compared with the initial situation (Fig. 9). The maximum horizontal displacements measured by the monitoring points ZH18 and ZH20 is increased by approximately 14.3% and 24.7%, respectively, but the value measured by the monitoring point ZH22 is decreased by 11.6%. At the inner strut depth of 6 m, the maximum horizontal displacements measured by the monitoring points ZH18 and ZH20 are decreased by approximately 6.7% and 6.2%, respectively, but the value measured by the monitoring point ZH22 is increased by 21.0%. In addition, as the strut depth changes from 0 m to 6 m, the horizontal displacement measured by the monitoring point ZH20 changes from a bow-shape to an S-shape, which shift the position of the maximum horizontal displacement downwards.

As shown in Fig. 10, when the depth of inner strut changes from 0 m to 6 m, the variation of maximum horizontal displacement measured by the monitoring point ZH22 is the largest, which is increased by 36.4%. The change of maximum horizontal displacement measured by the monitoring point ZH20 is the second, which is decreased by 27.8%, and the variation of maximum horizontal displacement measured by the monitoring point ZH18 is the smallest, which is decreased by 17.9%.

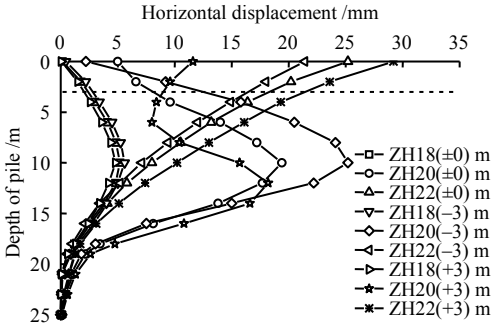

Fig. 9 Distributions of horizontal displacements of soldier piles at different strut positions

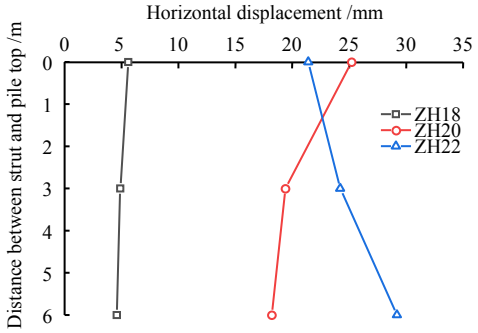

Fig. 10 Maximum horizontal displacements of soldier piles at different strut positions

5.2 Axial force of inner strut

As shown in Fig. 11, under the conditions of inner strut depths of 0 m, 3 m and 6 m, the axial force variations measured by the monitoring points ZC04, ZC05 and ZC06 increase nonlinearly with the excavation depth, and their growth rate gradually decreases. Thus, the downward movement of the strut position can significantly increase the axial force of inner struts. Compared with the original position, the maximum axial forces measured by the monitoring points ZC04, ZC05 and ZC06 are decreased by 10.7%, 10.0% and 12.1%, respectively, when the support depth is 0 m. However, the maximum axial forces measured by the monitoring points ZC04, ZC05 and ZC06 are increased by 32.7%, 31.3% and 34.2%, respectively, when the support depth is 6 m.

As shown in Fig, 12, it is obviously found that as the inner strut depth changes from 0 m to 6 m, the maximum axial forces measured by the monitoring points ZC04, ZC05 and ZC06 are increased by 49.2%, 45.5% and 42.4%, respectively.

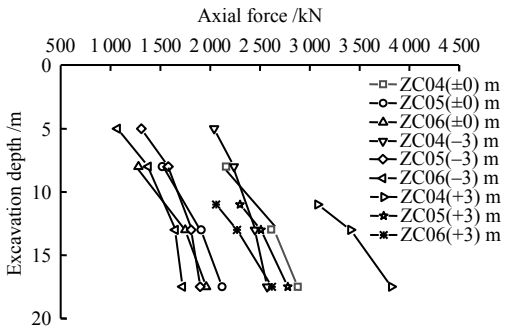

Fig. 11 Axial forces of strut at different strut positions

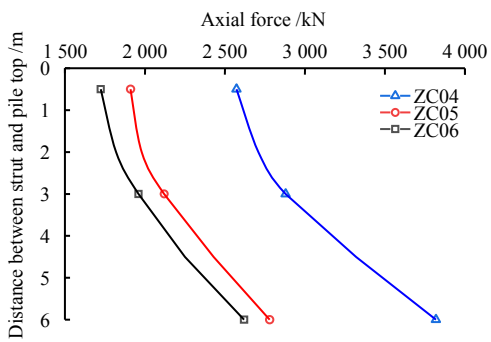

Fig. 12 Maximum axial forces of strut at different strut positions

5.3 Building settlement

The settlements of the building corners measured by the monitoring points CZ14, CZ15, CZ16 and CZ17 compared to the changes in the support position are shown in Fig. 13. It is found that the uneven settlement exists. The settlement measured by the monitoring point CZ17 is the largest, the settlement measured by the monitoring point CZ15 is the smallest, and the sequence for the settlement monitoring points is CZ17 > CZ15 > CZ16 > CZ14. Under the condition of inner strut depth of 0 m, the maximum settlements measured by the monitoring points CZ14, CZ15, CZ16 and CZ17 are increased by 8.1%, 11.2%, 13.5% and 18.7% compared with those of the original condition. Under the condition of inner strut depth of 6 m, the maximum values of settlement measured by the monitoring points CZ14 and CZ16 are increased by 5.8% and 13.5% compared with those of original condition. However, the values of the maximum settlement measured by the monitoring points CZ15 and CZ17 are decreased by 2.4% and 5.6% compared with those of original condition.

The maximum differential settlements at inner strut depths of 0 m, 3 m and 6 m are 5.61 mm, 4.44 mm and 3.40 mm, respectively. Accordingly, the total tilt rates of the building are 0.17‰, 0.13‰ and 0.10‰, which are less than 1/500 reported by Burland et al.[28] and 1/667 recommended by Wang et al.[29].

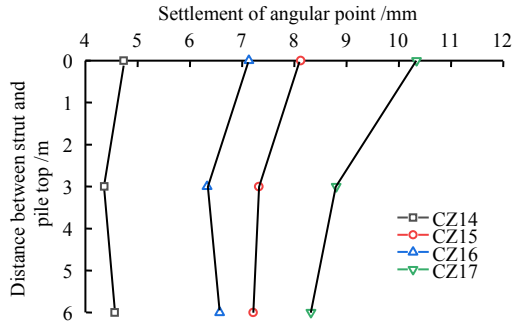

Fig. 13 Settlements of building corners at different strut positions

5.4 Lateral earth pressure of soldier piles

The lateral earth pressures of the soldier piles measured by the monitoring points ZH18, ZH20 and ZH22 compared to the changes in the support position are shown in Fig. 14. It is clearly found that there exists a neutral point approximately 2 m below the bottom of the foundation pit, where the lateral earth pressure is equivalent to the static earth pressure. The piles deform and rotate around the neutral point. Thus, above the neutral point, the lateral earth pressures of these piles are distributed in the interval of static earth pressure and active earth pressure. Another important area is below the neutral point, where the lateral earth pressures acting on these piles are distributed in the interval of static earth pressure and passive earth pressure. In addition, there is a sudden increase at the junction of the inner struts and piles, since the lateral displacement of soil near the inner strut is smaller than other area.

Under the condition of inner strut depth of 0 m (Fig. 14(a)), the lateral earth pressures acting on the pile measured by the monitoring point ZH18 are decreased by 12.5%, 13.6% and 14.3% at the depth of $0.25H_z$, $0.5H_z$ and $1.0H_z$, (H_z is the depth of pile within the depth range of the foundation pit, H_z= 13.0 m), respectively. However, the increments are 36.2% and 9.8% at the depths of $0H_z$ and $1.5H_z$, respectively. In addition, the lateral earth pressures acting on the pile measured by the monitoring point ZH20 are decreased by 13.3%, 14.5% and 15.8% at the depths of $0.25H_z$, $0.5H_z$ and $1.0H_z$, respectively. However, the increments are 51.0% and 10.2% at the depths of $0H_z$ and $1.5H_z$, respectively. Whereas, the lateral earth pressures acting on the pile measured by the monitoring point ZH22 are increased by 25.0%, 9.1%, 21.4% and 2.3% at the depths of $0H_z$, $0.25H_z$, $0.5H_z$ and $1.0H_z$, respectively. However, there is a 4.3% decrement at the depth of $1.5H_z$. Above the bottom of the foundation pit, the sequence of lateral earth pressure acting on the piles is ZH18 > ZH22 > ZH20.

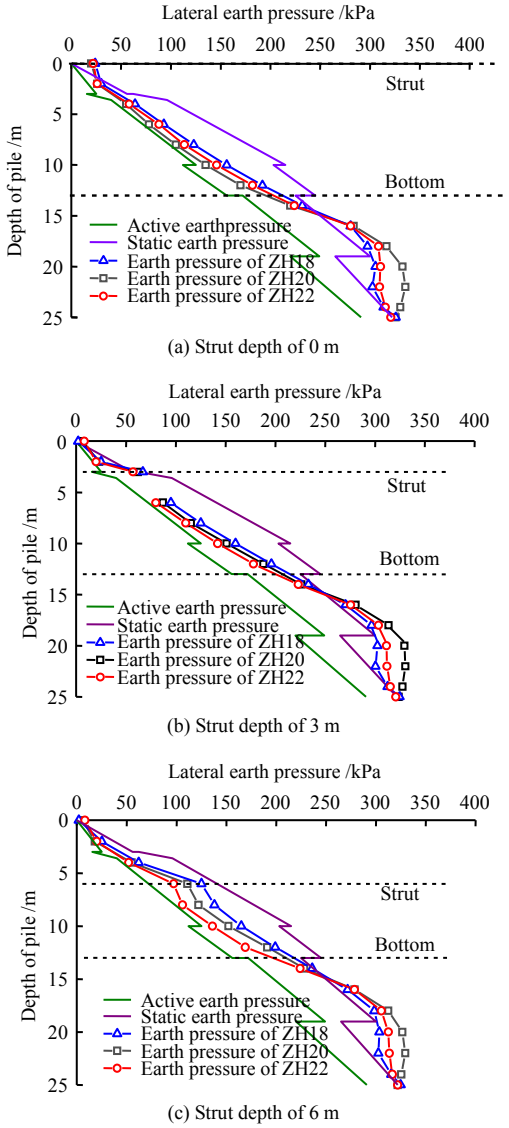

Fig. 14 Earth pressures of piles at different strut positions

Under the condition of inner strut depth of 6 m (Fig. 14(c)), the lateral earth pressures acting on the pile measured by the monitoring point ZH18 are increased by 9.2%, 13.5%, 32.4% and 11.0% at the depths of $0H_z$, $0.25H_z$, $0.5H_z$ and $1.0H_z$, respectively. However, there is a 13.1% decrement at the depth of $1.5H_z$. Additionally, the lateral earth pressures acting on the pile measured by the monitoring point ZH20 are increased by 1.3%, 35.2% and 23.1% at the depths of $0.25H_z$, $0.5H_z$ and $1.0H_z$, respectively. However, the increments are 10.8% and 12.4% at the depths of $0H_z$ and $1.5H_z$, respectively. The lateral earth pressures acting on the pile measured by the monitoring point ZH22 are decreased by 14.5%, 7.5% and 4.0% at the depths of $0H_z$, $0.25H_z$ and $1.0H_z$, respectively. However, there are 21.2% and 8.3% decrements at the depth of $0.5H_z$ and $1.5H_z$, respectively. Above the bottom of the foundation pit, the sequence of lateral earth pressure acting on the piles is ZH18 > ZH22 > ZH20.

5.5 Bending moment of soldier piles

The bending moments of these piles measured by the monitoring points ZH18, ZH20 and ZH22 compared to the changes in the support position are shown in Fig. 15. Above the bottom of foundation pit, these piles measured by the monitoring points ZH18, ZH20 and ZH22 mainly show positive bending moment. However, negative bending moment mainly shows below the bottom of foundation pit. As the strut position changes downwards, the positive bending state is changed from a bow-shape to a double bow-shape (wide at the bottom and narrow at the top), and the maximum positive bending moments measured by the monitoring points ZH18, ZH20 and ZH22 are increased. In addition, the position of the maximum positive bending moment occurs deeper. In addition, although the state of negative bending moment and the position of maximum negative bending moment of these piles almost remain stable, the maximum negative bending moments of these piles are decreased.

Under the condition of inner strut depth of 0 m (Fig. 15(a)), the maximum positive bending moments measured by the monitoring points ZH18, ZH20 and ZH22 are decreases by 11.7%, 13.0% and 15.9%, respectively, and the maximum negative bending moments measured by the monitoring points ZH18, ZH20 and ZH22 piles are increased by 21.0%, 15.3% and 13.7%, respectively, compared to the initial situation.

Under the condition of inner strut depth of 6 m (Fig. 15(c)), the maximum positive bending moments measured by the monitoring points ZH18, ZH20 and ZH22 piles are increased by 11.1%, 12.4% and 14.2%, respectively, and the maximum negative bending moments are decreased by 19.7%, 14.5% and 12.9%, respectively, compared to the initial situation.

6 Optimum inner strut position

6.1 Determination of optimum inner strut position

The maximum settlement of the adjacent building, the maximum horizontal displacement of the soldier pile, the maximum axial force of the inner strut, the maximum lateral earth pressure on the soldier piles above foundation pit, and the maximum bending moment in the soldier piles at original inner strut position are defined as s_{max}, x_{max}, F_{max}, p_{max} and M_{max}, respectively. The ratios of the variation values to the initial values under the conditions of different support positions are used to describe the sensitivity of the deformation and the force of adjacent building and foundation pit. The ratios are defined as K_s, K_x, K_F, K_p and K_M, respectively. The sensitive values of foundation pit and building at different strut positions are shown in Fig. 16.

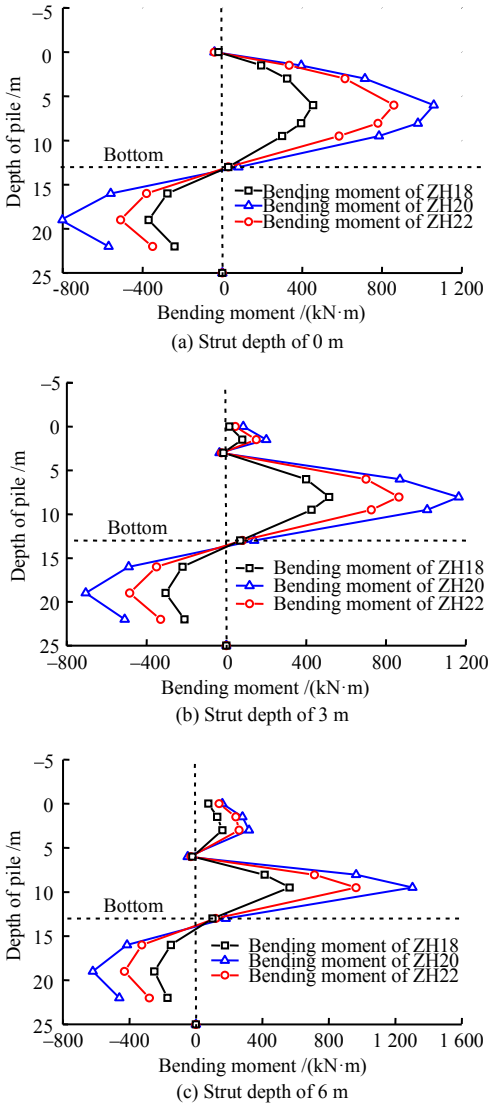

Fig. 15 Bending moments of piles at different strut positions

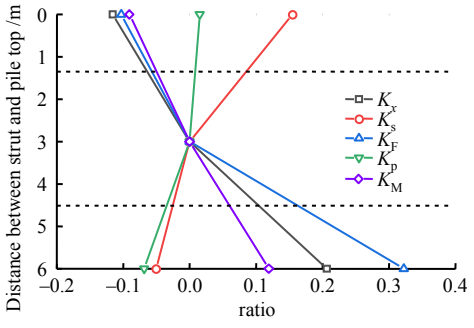

Fig. 16 Sensitivity values of foundation pit and adjacent building

As shown in Fig. 16, these sensitive values change nonlinearly as the strut position moves downwards. Generally, the sensitive values of K_s and K_p are decreased as the strut position moves downwards. In contrast, the sensitive values of K_x, K_F and K_M are increased. The ranges of K_x, K_s, K_F, K_p and K_M are –0.12 to 0.21, –0.05 to 0.16, –0.10 to 0.33, –0.07 to 0.02 and –0.09 to 0.06, respectively. By adjusting the position of inner strut, the sensitivity values of foundation pit and adjacent building can be controlled at –0.12 to 0.33. In this study, the optimal strut position is determined by the intersections of the sensitive values, and the optimal depth of the strut position is $0.10H_z$–$0.33H_z$ ($0.33H_e$–$0.50H_e$, $H_e = H_z + 4.5$). Accordingly, the sensitive value ranges from –0.07 to 0.15.

6.2 Relationship between deformation and strut position

The depth of strut position and tilt rate of the adjacent building are defined as t and K_q, respectively. The maximum horizontal displacement of foundation pit, maximum settlement and tilt rate of the building under different strut positions are shown in Figs. 17 and 18.

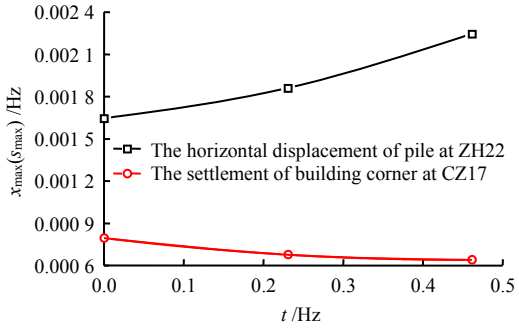

Fig. 17 Relationships of horizontal displacement of foundation pit and/or settlement of building with strut depth

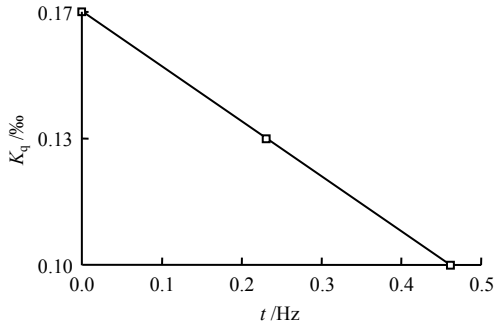

Fig. 18 Relationship between tilt rate of the building and strut depth

The maximum horizontal displacement of the foundation pit increases nonlinearly as the strut position moves downwards. However, the maximum settlement of the building decreases nonlinearly. Accordingly, the tilt rate of the building changes linearly as the strut position moves downwards.

Due to the nonlinear relationship of the horizontal displacement of foundation pit and the strut depth, the points in Figs. 17 and 18 are calculated in terms of power function, exponential function and logarithmic function. Finally, it is found that their relationships conform to the exponential form of quadratic equation with one variable. In a similar way, the relationship between the settlement of the adjacent building and the strut depth conforms to the exponential form of quadratic equation with one variable too. However, the relationship between the tilt rate of the adjacent building and the strut depth conforms to the exponential form of linear equation with one variable. These relationships are as follows:

$$\frac{x_{max}}{H_z} = 1.6\left(\frac{t}{H_z}\right)^2 + 0.6\frac{t}{H_z} + 1.65 \quad (1)$$

$$\frac{s_{max}}{H_z} = 0.77\left(\frac{t}{H_z}\right)^2 - 0.7\frac{t}{H_z} + 0.79 \quad (2)$$

$$K_q = -0.15\frac{t}{H_z} + 0.17\text{‰} \quad (3)$$

7 Conclusions

In this analysis, the impact laws of inner strut position variation on the stress and deformation characteristics of the convex corner foundation pit with adjacent loads were investigated by field monitoring and numerical simulation. The findings can be summarized as follows:

(1) From the point of deformation, the influence of inner strut position on the horizontal displacement of foundation pit is larger than that of the settlement of the adjacent building. It is beneficial to the settlement and tilt rate of the building as the depth of strut position increases, although the horizontal displacement of foundation pit is increased.

(2) From the mechanical point of view, the variation of soldier depth has the largest effect on the axial force of inner struts and the smallest effect on the lateral earth pressure. The lateral earth pressure is not sensitive to the inner strut depth. It is beneficial to the bending moment of soldier piles and the axial force of inner struts as the struts move upwards.

(3) The optimal strut position in this analysis is between $0.10H_z$ and $0.33H_z$, and the maximum horizontal displacement of foundation pit increases nonlinearly as the strut position moves downwards. However, the maximum settlement of the building decreases nonlinearly. In addition, the tilt rate of the building decreases linearly as the strut depth increases.

Declaration of competing interest

The authors declare that they have no known competing financial interests or personal relationships that could have appeared to influence the work reported in this paper.

References

[1] SUN Y Y, XIAO H J. Wall displacement and ground-surface settlement caused by pit-in-pit foundation pit in soft clays[J]. KSCE Journal of Civil Engineering, 2021,

25(4): 1262–1275.

[2] ZHAO J P, TAN Z S, YU R S, et al. Deformation responses of the foundation pit construction of the urban metro station: a case study in Xiamen[J]. Tunneling and Underground Space Technology, 2022, 128: 104662.

[3] PECK R B. Deep excavation and tunneling in soft ground[C]//Proceedings of the 7th International Conference on Soil Mechanics and Foundation Engineering. Mexico City: [s. n.], 1969: 225–290.

[4] LIU R. Deformation caused by excavation of foundation pit and its influence on adjacent buildings[D]. Beijing: Beijing Jiaotong University, 2015.

[5] BOONE S J. Ground-movement-related building damage[J]. Journal of Geotechnical Engineering, 1996, 122(11): 886–896.

[6] SCHUSTER M, KUNG G T, JUANG C H, et al. Simplified model for evaluating damage potential of buildings adjacent to a braced excavation[J]. Journal of Geotechnical and Geoenvironmental Engineering, 2009, 135(12): 1823–1835.

[7] FINNO R J, BRYSON L S. Response of building adjacent to stiff excavation support system in soft clay[J]. Journal of Performance of Constructed Facilities, 2002, 16(1): 10 –20.

[8] WU Feng-bo, JIN Huai, ZHU Shao-kun. Surface deformation characteristics of Beijing Rail Transit foundation pit engineering[J]. Rock and Soil Mechanics, 2016, 37(4): 1066–1074.

[9] HSIAO E C, SCHUSTER M, JUANG C H, et al. Reliability analysis and updating of excavation-induced ground settlement for building serviceability assessment[J]. Journal of Geotechnical and Geoenvironmental Engineering, 2008, 134(10): 1448–1458.

[10] KUNG G T, JUANG C H, HSIAO E C, et al. Simplified model for wall deflection and ground-surface settlement caused by braced excavation in clays[J]. Journal of Geotechnical and Geoenvironmental Engineering, 2007, 133(6): 731–747.

[11] CHENG Y, WANG Y H. Analysis of interaction between deep foundation pit in soft soil and adjacent metro station[J]. Urban Rail Transit Research, 2019, 22(9): 14–20.

[12] GOH A T C, WONG K S, TEH C I, et al. Pile response adjacent to braced excavation[J]. Journal of Geotechnical and Geoenvironmental Engineering, 2003, 129(4): 383–386.

[13] WANG Jun-feng, KOU Xiao-yong, SUN Jian, et al. Research on the space effect of the deep foundation pit with double-row piles supporting structure[J]. Building Structure, 2022, 52(Suppl.1): 2483–2490.

[14] SONG Zhuo-hua, ZHANG Ke-sheng, ZHAI Hao-bo, et al. Analysis on deformation characteristics of diaphragm wall at external corner of deep foundation pit in soft soil stratum[J]. Building Structure, 2022, 52(Suppl.): 2491–2496.

[15] WU Zhi-min, TU Yu-min. Space effect of soil-nailing excavation protection[J]. Rock and Soil Mechanics, 2007, 28(10): 2178–2182.

[16] PAN Hong, ZHOU Chen-fa, CAO Hong. Analysis of spatial effect and deformation of corner of composite soil nailing walls[J]. Rock and Soil Mechanics, 2008, 29(2): 333–336.

[17] YE H L. A three-in-one structure of foundation pit support inner support system and basement structure system: CN210507463U[P]. 2020-05-12.

[18] YAN Teng-fei, CHEN Bao-guo, ZHANG Lei, et al. Dynamic adjustment method of diaphragm wall supporting system in deep foundation pit and its application[J]. Journal of Zhejiang University (Engineering Science), 2022, 56(2): 356–367.

[19] CHEN B G, YAN T F, SONG D B, et al. Experimental investigations on a deep excavation support system with adjustable strut length[J]. Tunnelling and Underground Space Technology, 2021, 115: 104046.

[20] CHEN Bao-guo, YAN Teng-fei, WANG Cheng-peng, et al. Experimental study on compatible deformation of diaphragm wall support system for deep foundation pit[J]. Rock and Soil Mechanics, 2020, 41(10): 3289–3299.

[21] QIAO Ya-fei, DING Wen-qi, WANG Jun, et al. Deformation characteristics of deep excavations for metro station in Wuxi[J]. Chinese Journal of Geotechnical Engineering, 2012, 34(Suppl.): 761–766.

[22] ZHANG Tu-qiao, ZHANG Yi-ping, GONG Xiao-nan. Behavior analysis of single strut arched retaining structure in foundation pits[J]. Chinese Journal of Geotechnical Engineering, 2001, 33(1): 99–103.

[23] LIU Run, YAN Yue, YAN Shu-wang. Stability analysis of foundation pit with position change of braces[J]. Chinese Journal of Rock Mechanics and Engineering, 2006, 35(1):174–178.

[24] JIANG A, QIU M, WU B, et al. Research on the deformation of deep foundation excavation supports and its control measures[J]. Construction Technology, 2013, 42(1): 59–64.

[25] GAO X J, LEI J, MA Z. Analysis on axial force of concrete support for half covered deep foundation pit of subway station[J]. Science Technology and Engineering, 2021, 21(30): 13054–13060.

[26] XIE Q, CAO Z L, SUN W C, et al. Numerical simulation of the fluid-solid coupling mechanism of water and mud inrush in a water-rich fault tunnel[J]. Tunnelling and Underground Space Technology, 2022, 131: 104796.

[27] VENKATESAN G, MURUGAN C A, ISAC S J, et al. Experimental investigation on load carrying capacity of hollow and composite pile materials in layered soil[J]. Materials Today: Proceedings, 2022, 65(9): 3951–3958.

[28] BURLAND J B, WROTH C. Settlement of buildings and associated damage[C]//Proceedings of Conference on Settlement of structures. Cambridge: Halsted Press, 1974.

[29] XU Zhong-hua, WANG Wei-dong, WANG Jian-hua. Responses of heritage buildings to an adjacent deep excavation using top-down method[J]. China Civil Engineering Journal, 2009, 42(10): 88–96.